

# Predicting Blood Pressures for Pregnant Women by PPG and Personalized Deep Learning

Duc Huy Nguyen<sup>ID</sup>, Paul C.-P. Chao<sup>ID</sup>, Fellow, IEEE, Hiu Fai Yan<sup>ID</sup>, Tse-Yi Tu<sup>ID</sup>, Chin-Hung Cheng<sup>ID</sup>, and Tan-Phat Phan<sup>ID</sup>

**Abstract**—Blood pressure (BP) is predicted by this effort based on photoplethysmography (PPG) data to provide effective pre-warning of possible preeclampsia of pregnant women. Towards frequent BP measurement, a PPG sensor device is utilized in this study as a solution to offer continuous, cuffless blood pressure monitoring frequently for pregnant women. PPG data were collected using a flexible sensor patch from the wrist arteries of 194 subjects, which included 154 normal individuals and 40 pregnant women. Deep-learning models in 3 stages were built and trained to predict BP. The first stage involves developing a baseline deep-learning BP model using a dataset from common subjects. In the 2<sup>nd</sup> stage, this model was fine-tuned with data from pregnant women, using a 1-Dimensional Convolutional Neural Network (1D-CNN) with Convolutional Block Attention Module (CBAMs), followed by bi-directional Gated Recurrent Units (GRUs) layers and attention layers. The fine-tuned model results in a mean error (ME) of  $-1.40 \pm 7.15$  (standard deviation, SD) for systolic blood pressure (SBP) and  $-0.44$  (ME)  $\pm 5.06$  (SD) for diastolic blood pressure (DBP). At the final stage is the personalization for individual pregnant women using transfer learning again, enhancing further the model accuracy to  $-0.17$  (ME)  $\pm 1.45$  (SD) for SBP and  $0.27$  (ME)  $\pm 0.64$  (SD) for DBP showing a promising solution for continuous, non-invasive BP monitoring in precision by the proposed 3-stage of modeling, fine-tuning and personalization.

Received 15 June 2023; revised 25 February 2024; accepted 5 April 2024. Date of publication 10 April 2024; date of current version 8 January 2025. This work was supported in part by the National Science and Technology Council under Grant 113-2923-E-A49-006, Grant 111-2221-E-A49-159-MY3, Grant 112-2811-E-A49-508 -MY2, and Grant 112-2223-E-A49-006, and in part by the Hsinchu and Southern Taiwan Science Park Bureaus, Ministry of Science and Technology, Taiwan under Grant 110CE-2-02 and Grant 112AO28B. (Corresponding author: Paul C.-P. Chao.)

This work involved human subjects or animals in its research. Approval of all ethical and experimental procedures and protocols was granted by the National Taiwan University Hospital (NTUH) under Application No. CS2-21096, and performed in line with the Institutional Review Board (IRB) at National Taiwan University Hospital (NTUH).

Duc Huy Nguyen and Paul C.-P. Chao are with the Department of Electrical and Computer Engineering, National Yang Ming Chiao Tung University, Hsinchu 30010, Taiwan (e-mail: ndhuyvn1994@gmail.com; pchao@ncyu.edu.tw).

Hiu Fai Yan is with the Department of Electronics and Electrical Engineering, National Yang Ming Chiao Tung University, Hsinchu 30010, Taiwan (e-mail: qaz11328.eed09g@ntcu.edu.tw).

Tse-Yi Tu is with the Department of Mechanical Engineering, Chun Yuan Christian University, Taoyuan 320314, Taiwan (e-mail: ann@cycu.edu.tw).

Chin-Hung Cheng and Tan-Phat Phan are with the Amengine Corp., Zhubei 302058, Taiwan (e-mail: chinhung.cheng@gmail.com; phantan-phat512@gmail.com).

Digital Object Identifier 10.1109/JBHI.2024.3386707

**Index Terms**—Cuffless blood pressure (BP), preeclampsia, photoplethysmography (PPG), transfer learning, pregnant women, personalization.

## I. INTRODUCTION

PREECLAMPSIA is a potentially fatal disease that affects pregnant women, causing serious issues for both the mother and the fetus [1], [2]. Although the reason for preeclampsia is still undetermined by other researchers [3], its symptoms, including gestational hypertensive disorder, proteinuria and/or sudden rises in blood pressure (BP), are used for diagnosis. Symptoms of preeclampsia usually occur in the early stages of pregnancy, with more severe consequences coming at 20 weeks later [4]. Early diagnosis and medical treatment are crucial to address the disease. To this end, rises in blood pressure (BP) and/or gestational hypertensive disorders during pregnancy [5] are considered important signs in prenatal health monitoring as valid preludes to preeclampsia. While conventional methods for monitoring gestational hypertensive disorders require the use of a cuffed blood pressure monitor, the limitations of this device make it unsuitable for long-term use. As for monitoring BP alone, the difficulty also exists due to “white coat” effect [6], [7], [8]. Experiments have found that the presence of a doctor may cause an increase in a patient’s blood pressure due to the “white coat” effect [6], [7], [8]. Therefore, BP measurements taken during prenatal screening may not truly reflect the situation, not to mention that there may be a difference or variability between daytime and nighttime blood pressure values measured from the patient [9], [10], [11]. Therefore, monitoring BPs continuously for 24 hours becomes an imminent task to track changes in a pregnant woman’s blood pressure for ensuring the health of both the mother’s heart and the fetus’s growth.

Continuous BP monitoring holds a vital role in prenatal care, particularly for pregnant women who are at risk of hypertensive disorders like preeclampsia. These conditions require observation to manage maternal health effectively. Despite its importance, the development of methods for continuous BP monitoring in this population has not been extensively explored in the research community. Current approaches practiced for monitoring BP are often intermittent measurements with cuff-based sphygmomanometers, which can be cumbersome and fail to capture fluctuations in blood pressure that are of clinical importance during pregnancy. Such methods are less feasible for continuous

monitoring, which is essential for tracking BP, and particularly detecting sleep-time hypertension that are critical for assessing the risk of preeclampsia. Only limited reported works attempted to address this issue, such as those in [12], [13], [14], [15] where striving to conduct continuous monitoring on bio-signals like heart rate variability (HRV) and/or BP frequently; however, but their reliance on conventional cuff-based monitors hinders their application during periods of rest and sleep. In particular, Gupta et al. [15] proposed to utilize a wearable photoplethysmography (PPG) sensor to provide HRV for health monitoring but no BPs provided. Note that PPG is a well-known optical bio-sensing method to detect effective blood vessel pulsation thanks to the merit of non-invasiveness [16]. This non-invasiveness makes PPG sensors suitable to realize cuffless BP monitoring for long, continuous time. Nowadays, PPG sensors are considered already reliable in many portable medical devices and smartwatches to measure heart rate [17], while vast amount of reported research works have agreed with the potential of using the PPG devices to accomplish continuous monitoring of BP [18], [19], [20], [21], [22]. In this study, effort is dedicated for pregnant women to use the PPG technology to monitor BPs continuously, capable of distilling feasible pre-warning for preeclampsia.

Based on PPG signals measured by the patch, algorithms of pre-signal processing, quality-check and deep-learning models are developed to predict BPs. Note that to date many learning machines including deep learnings have been developed based on PPG for heart rate regression [23], [24], predicting BPs [14], [15], [16], and classification problems like detecting atrial fibrillation [25], [26]. The effort herein is dedicated to monitor BP continuously for pregnant women based on PPG. Having established the deep-learning model for predicting BP based on PPG data from generic patients, the model is next transferred for pregnant women and further personalized for individual pregnant woman to aim for the highest accuracy possible. This study presents for the first time a three-stage modeling for BP prediction, including the development of a baseline model from generic population, fine-tuning of the baseline, and the personalization on the fine-tuned model for individual pregnant women to enhance accuracy. Through 3 stages, this work offers a chance to improve the accuracy of BP prediction for an individual by a personalized model.

## II. MATERIAL AND METHOD

The cuffless PPG patch developed by Pandey and Chao [27], as shown in Fig. 1, is used to collect PPG data for BP estimation, with the process outlined in Fig. 2 and presented in the subsequent subsections. The continuous BP monitoring for pregnant women is developed herein by this new PPG patch to collect PPG data and to build accompanying algorithms to predict BPs. The afore-mentioned PPG sensor patch is able to conduct cuffless blood pressure measurement on pregnant women without difficulty and discomfort.

### A. Data Collection

The PPG signals in this study were acquired using sensors from the Intelligent Sensing Lab at National Yang Ming Chiao

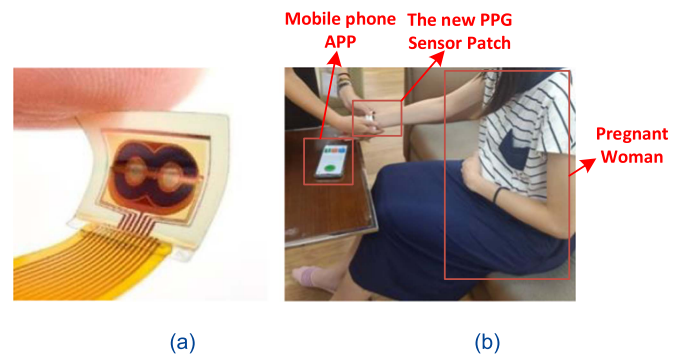


**Fig. 1.** (a) The flexible PPG sensor patch [25]; (b) BP measurement on a pregnant woman using the PPG sensor patch.

**TABLE I**  
CHARACTERISTICS OF COLLECTED DATA FROM TWO DATABASES

	Database 1	Database 2
<b>Patient group</b>	Men, Women	Pregnant women
<b>Age range</b>	19 to 89	22 to 41
<b>SBP range</b>	80 to 184	94 to 147
<b>DBP range</b>	50 to 119	50 to 94
<b>Number of subjects</b>	154	40
<b>Number of data</b>	2039	648
<b>Sampling rate</b>	1000Hz	250Hz
<b>Place of data collection</b>	National Taiwan University Hospital	Jin-Sin Women and children hospital
<b>Used model</b>	Pre-trained, baseline model	Finetune model, personalized model

Tung University [27]. The data collection was approved by the Institutional Review Board (IRB) numbered CS2-21096. A total of 154 patients from National Taiwan University Hospital (NTUH) participated, with ages ranging from 19 to 89, and diverse genders, weights, and blood pressure values, also 40 pregnant women from the Jin-Sin Women and Children Hospital for this research effort. Each participant was subjected to 2 to 3 measurement sessions, collectively yielding a dataset of 456 waveforms, which provide the basis for the analysis. During each measurement, the patient's blood pressure was measured first using a traditional cuffed BP monitor BP7200 [28] developed by OMRON Healthcare, Inc, with BPs obtained from the cuffed device serving as the gold standards for the study. Table I presents the two databases used in the pre-trained (baseline) and fine-tuned models, with the database collected from generic, normal population at NTUH using a 1000-Hz-sampling PPG patch, while the fine-tuned database collected from pregnant women using a 250 Hz PPG patch. The SBP and DBP values of the patients were also measured by BP-7200 to evaluate the model's performance.

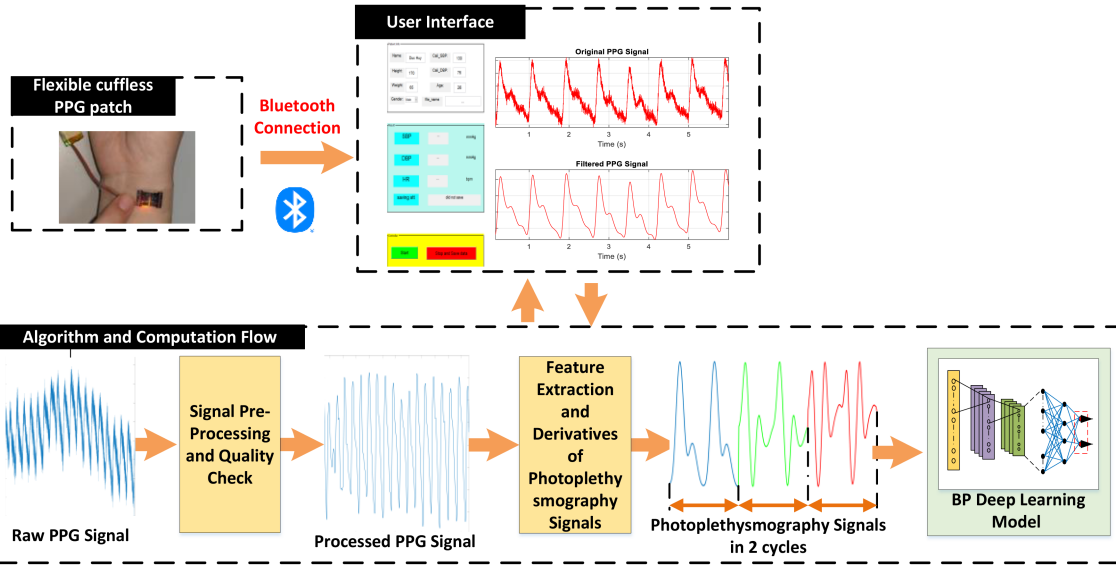


Fig. 2. Generic computation flow of BP prediction based on PPG signals.

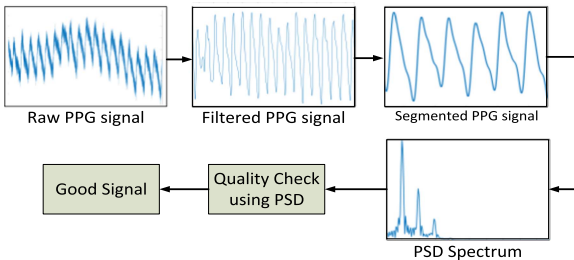


Fig. 3. Process of data filtering and screening process.

### B. Signal Pre-Processing and Quality Check

The filtering process on the measured raw PPG is illustrated by Fig. 3. Initially, the raw PPG signals were collected and filtered using a Butterworth bandpass filter with a 0.5–5 Hz passband. Subsequently, the filtered signals were segmented into 6-second windows. Each segment was then evaluated using a power spectral density (PSD) [29] to determine its quality. It is worth noting herein that during data collection, the PPG sensing patch may have received noise from various sources, such as internal components, ambient light, or patient movement, which can affect signal quality, reducing the accuracy of the deep learning model [30], [31], [32], [33], [34]. Thus, several past studies have reported the development of PPG sensors that are immune to motion artifact and other types of noise using different hardware or components [35], [36], [37], [38]. To eliminate noise, a 4<sup>th</sup>-order Butterworth bandpass filter was designed and employed in this study as it has been demonstrated to be a simple and effective technique for PPG noise cancellation in some previous studies [39], [40], [41], [42]. The passband was set to 0.5–5 Hz to retain all peaks and notches of the PPG waveforms while removing high frequency noise and low frequency DC drifting. Next, the filtered PPG signals underwent screening based on their PSDs derived via fast Fourier transform (FFT). The checks on PSD

was conducted using a criterion of 0.15, which implies that the ratio of the harmonics from the PPG peaks must be greater than 15% of the entire sequence. For PPG signals with a PSD value above 0.15, the peaks and harmonics of the signals were apparent in both the time and frequency domains, indicating that these signals are suitable for the deep learning model. Note that a single PPG waveform may contain parts of both qualified and non-qualified signals, while its PSD value may be large enough to pass the PSD check, but non-qualified parts will not be considered as inputs to the subsequent deep learning model built for predicting BPs.

### C. Derivatives of Photoplethysmography Signals as Inputs

Features are extracted from qualified PPG signals towards BP prediction. Derivatives of PPG signals such as Velocity Plethysmogram (VPG) and Acceleration Plethysmogram (APG) are considered as inputs to the model built later for providing effective insights towards precision blood pressure prediction [43], [44]. VPG as the first derivative of the PPG signal is calculated by

$$VPG = \frac{d(PPG)}{dt} \quad (1)$$

Similarly, APG as the second derivative of the PPG signal is derived by

$$APG = \frac{d^2(PPG)}{dt^2} \quad (2)$$

The derivatives in (1), (2) are used as inputs to the deep learning (DL) models developed later for identifying and extracting the PPG signal's key features, like systolic peaks, dicrotic notches and peaks [45], [46]. Thus, the proposed DL models to be built later will incorporate PPG, VPG, and APG as the inputs as seen in Fig. 4, utilizing their distinct characteristics to achieve precision BP prediction.

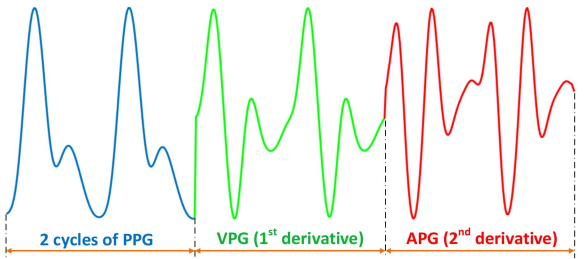


**Fig. 4.** Organization of PPG signals, where the original measured, 1<sup>st</sup> and 2<sup>nd</sup> derivatives are used as inputs to the BP prediction model.

In this study, the PPG signals used for the pre-trained (baseline) model were obtained from healthy individuals at a sampling frequency of 1000 Hz. The filtered signals were divided into 2-cycle segments, which were resampled to 1000 sample points. The resulting segments, together with their first and second derivatives, were normalized using min-max normalization as

$$x_{scaled} = \frac{x - x_{\min}}{x_{\max} - x_{\min}} \quad (3)$$

Subsequently, the sequence was concatenated into a (1000x3) data input for the deep learning model.

#### D. Deep Learning Models

The pre-processing of data preparation and train-test split for the proposed deep learning (DL) model to predict BPs is elaborated in this section. The computation flow consist of 3 steps, data collection, signal pre-processing, and a deep learning model. Fig. 5 provides an overview of the data preparation and train-test split. The collected databases underwent pre-processing, shuffling, and division into two sets, one for generic, normal individuals while another for pregnant women. Next, a generic DL model was built based on the whole database as a pre-trained baseline model, and then fine-tuned based on the data collected from pregnant women except for those of selected three pregnant women. Lastly, the data of the selected three pregnant women are used to build the final personalized BP prediction models for them individually.

**1) Baseline Model Architecture:** Fig. 6(a) shows the proposed architecture of a DL model, which consists of two 1-Dimensional Convolutional Neural Network (1D-CNN) blocks with Convolutional Block Attention Modules (CBAMs) [47] for feature extraction to enhance accuracy. In this model, two bi-directional Gated Recurrent Unit (GRU) layers, two attention layers and a GRU layer are employed to analyze the timing relationship of the extracted features. The model is connected to two dense layers separately, where the biological information of the subject is incorporated, including gender, age, height, weight, the length of the 2-cycle input PPG waveform. The layers eventually output the Systolic Blood Pressure (SBP) and Diastolic Blood Pressure (DBP). This proposed architecture makes possible the capture of distinct patterns associated with each parameter, mitigating potential biases/trade-offs that may arise when using a single layer for simultaneous SBP and DBP prediction, thus achieving a satisfactory balance between

accuracy for SBP and DBP. In this way, its adaptability and robustness across the regressions can be enhanced.

On the proposed architecture shown in Fig. 6 also, 1D-CNN blocks are designed to handle the input raw PPGs undergoes, since 1D-CNN blocks are intrinsically adept at handling time-series data. Each 1D-CNN block is enhanced with a CBAM, providing a dual mechanism to focus the model on the most informative features. The CBAM augments feature extraction by applying both channel and spatial attention sequentially, leading to a refined feature map that emphasizes salient features while suppressing less useful information. After the CNN layers, two bi-directional GRU layers are employed. These layers are pivotal for capturing the dynamic temporal dependencies within the PPG waveform, owing to their ability to preserve information over extended sequences in both forward and reverse temporal directions. Two attention layers follow the GRU layers, providing the model with a mechanism to weigh the importance of different temporal segments of the PPG signal. This selective attention further enhances the model's ability to focus on periods of the signal that are most indicative of systolic and diastolic pressure variations. The final GRU layer serves to consolidate the temporal information, preparing the data for the subsequent dense layers. In this stage, the model integrates subject-specific biological parameters gender, age, height, weight, and the original length of the 2-cycle PPG waveform into two separate dense layers. This integration is crucial as these biological factors are known to influence blood pressure readings and their inclusion is expected to improve the model's accuracy. Finally, two values of SBP and DBP are delivered as outputs. Note that these outputs are the result of the model's comprehensive analysis of both the extracted features and the biological information of the subject, giving a strong chance of precision prediction.

In-depth design rationales behind the proposed DL architecture are provided herein. The 1D-CNN is adopted to automatically extract the spatial features of one-dimensional raw measured PPG waveforms over time. The machine-trained kernel in the 1D-CNN slides through the input signal in only one direction to perform convolution and extract features. The CBAM mechanism on the other hand uses a simpler method to first pool the convolutional output and then calculate the spatial/channel weights, thereby enhancing the spatial and channel-wise attention of the model. Also, the attention mechanism employed along with the bidirectional GRU layers is the standard dot-product (scaled dot-product) attention, a concept introduced and elaborated by Vaswani et al. [48]. This special attention was chosen due to its proven effectiveness in sequence-to-sequence models, where accurately capturing temporal relationships in data is of critical importance. In our implementation, the dot-product attention calculates alignment scores between each sequence element output by the GRU and a query, which, in this case, is also derived from the GRU outputs. This allows the model to dynamically focus on different parts of the input sequence for each output sequence element, thus capturing temporal dependencies with greater efficacy. The use of the dot-product attention mechanism is especially apt for our application, aligning well with the nature of the PPG signals. These signals are inherently sequential and contain vital temporal information indicative of the subject's

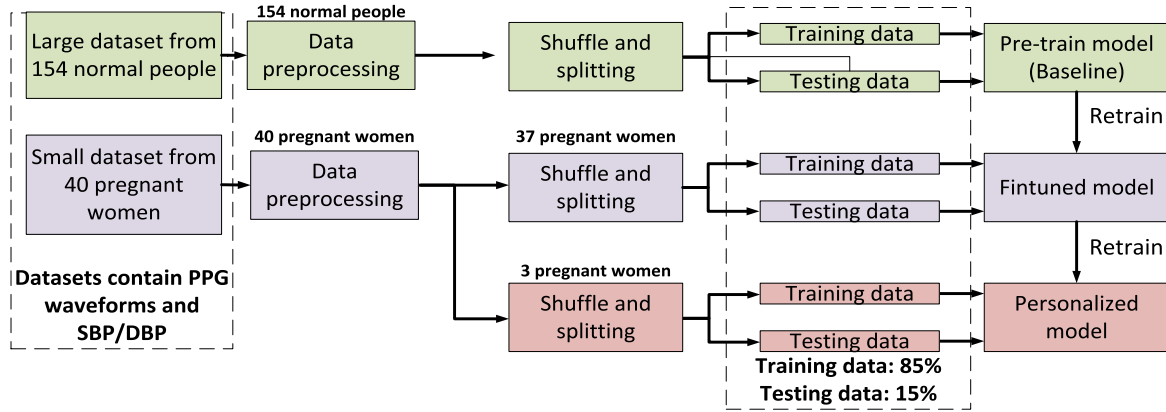


**Fig. 5.** Proposed data preparation and training flow for 3 deep-learning models that deliver the proposed 3-stage personalized BP prediction.

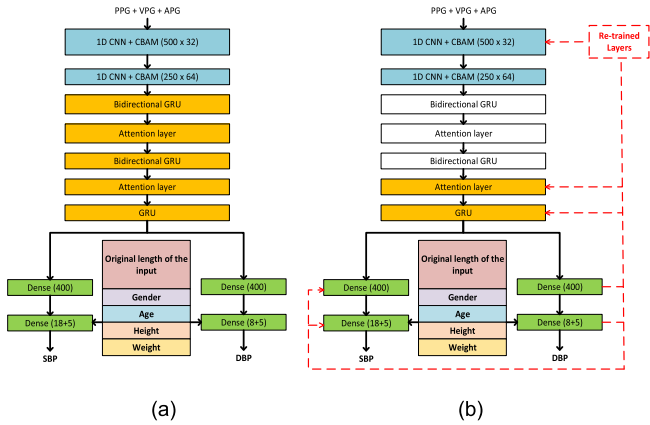


**Fig. 6.** (a) The proposed architecture of the deep learning model; (b) fine-tuning using transfer learning.

physiological state. By leveraging dot-product attention, our model can selectively emphasize different parts of the PPG signal, thereby enhancing its ability to extract meaningful features for blood pressure prediction, much analogous to the attention modules proposed by Woo et al.'s [47].

**2) Fine-Tuned Model for Pregnant Women Only:** As the data of pregnant women was collected from a different group of individuals with a different sensor hardware operated at a distinct sampling frequency, the pre-trained baseline model cannot be directly applied to the pregnant women. On the other hand, the available data from pregnant women alone are inadequate in amount for building a new model to deliver required accuracy, since it may lead to overfitting. To overcome this difficulty, the technique of transfer learning is adopted herein, as shown in Fig. 6(b), where most layers of the pre-trained model are fixed while only a few layers are retrained using the new, few data. This approach can fine-tune the pre-trained BP model to a new one specialized for pregnant women while using only a limited amount of data from pregnant patients. Next, towards personalization, multiple measured PPG data of an individual pregnant woman can be used further to train again the aforementioned fine-tuned model of pregnant women to arrive at even higher-precision for individual BP prediction. The approach of this personalization was also reported in [49], but not the same

as a whole as this work of the proposed 3-stage models for BPs of pregnant women.

**3) Personalized Model for Individual Woman:** Personalized models using transfer learning are developed and implemented individually for 3 pregnant women to validate the effectiveness of the proposed 3-stage BP model. As mentioned earlier, transfer learning can be used to fine-tune the pre-trained baseline BP model with only a few data from pregnant patients to specialize the model for pregnant women. However, the data from a single pregnant woman may not be sufficient to fully capture the unique relationship between PPG signal and BP value for that individual. Therefore, with leaving individual pregnant women left out from the 2<sup>nd</sup>-stage fine-tuning process, a second round of transfer learning (the 3<sup>rd</sup> stage actually) can be conducted using only the data from the selected individual woman to personalize the model for her alone. This approach can improve the accuracy of the prediction by accounting for her individual, unique characteristics in the relationship between PPG signal and blood pressure value in pregnant women. The personalized model is surely beneficial to high-risk pregnant women, such as those with gestational hypertension or preeclampsia, as it can provide more accurate, tailored and continuous predictions of BPs

**4) Training on Models:** The collected dataset, consisting of 456 waveform files, was randomly divided into a training set (85%) and a testing set (15%), resulting in 1580 training and 439 testing samples. The known K-fold cross validation was applied to finalize model parameters. K in K-fold cross validation was set to 5 as it provides a needed balance between preventing overfitting and reducing overall training time. This process involves dividing the training set into five equal subsets. In each of the five iterations for the afore-mentioned K-fold cross validation, one subset served as the validation set, while the remaining four were for training via cross-validation. The model's performance was then evaluated on the testing set to select the best-performing model. This method ensured effective learning and generalization to new data.

For the regression task of predicting BP, the Mean Square Error (MSE) was employed as the loss function in the deep learning model. Considering the model's complexity and the extensive number of parameters, the Adam optimizer was selected over traditional options like stochastic gradient descent

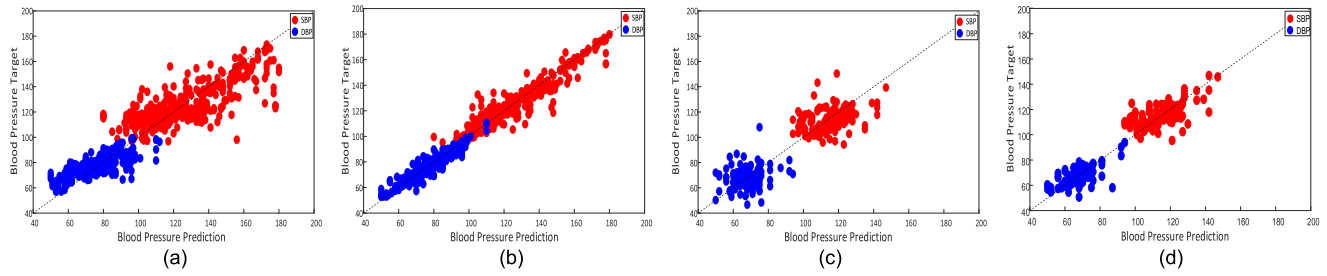


**Fig. 7.** Correlation plots for SBP and DBP predictions showing (a) baseline model without personal information, (b) baseline model with personal information, (c) model trained exclusively on pregnant women's database with personal information, and (d) finetuned model using pregnant women's database based on baseline training with personal information.

(SGD). This choice is due to Adam's incorporation of a momentum mechanism for faster convergence and its adaptive learning rate feature to ensure a smoother training process.

### III. RESULT AND VALIDATION

#### A. Result of the Baseline BP Model

The performance of the pre-trained, baseline DL model is evaluated herein based on training and validation results, to select the best model for subsequent fine-tunings to build the fine-tuned model for pregnant women only. Towards ensure favorable performance of the baseline BP model, the performance is also compared to those by the models from reported research works. For evaluating the accuracy and consistency of the BP prediction model, this study employs two complementary approaches including the Pearson correlation plot [50], [51] and the Bland-Altman plot [52]. The Pearson correlation plot serves as a measure of the linear relationship between the predicted and the reference blood pressure values, with a coefficient of 1 denoting perfect positive correlation while 0 indicates no linear correlation. This coefficient provides insight into the accuracy of the model's predictions in terms of their direction and strength relative to true values. On the other hand, the Bland-Altman plot is utilized to assess the built model by plotting the difference between the predicted and true values against their average. This method highlights the consistency and bias of the predictions across the range of measurements, which is critical for clinical validation. It can decipher the systematic errors that the model may have, which is not apparent from correlation alone. Thus, while the correlation plot assesses the model's accuracy, the Bland-Altman plot evaluates the model's consistency, both of which are essential for comprehensive performance evaluation.

Results of BP prediction for models are presented in Fig. 7. The pre-trained model based on generic, normal people without using personal information as inputs shows correlation values of 0.76 for SBP and 0.718 for DBP. The MAE results at 14.69 mmHg for SBP and 7.61 mmHg for DBP, with SDs of 11.06 mmHg for SBP and 6.08 mmHg for DBP. The respective correlation plot and Bland-Altman plots for this model are presented in Fig. 7(a) and Fig. 8(a), (e), respectively. On the other hand, the pre-trained model incorporating personal information achieves Pearson correlation values of 0.963 for SBP and 0.950 for DBP. The related correlation plot is depicted in Fig. 7(b), while the Bland-Altman plots in Fig. 8(b), (f)

**TABLE II**  
RESULTED DISTRIBUTION PERCENTAGES BY BASELINE MODEL AS OPPOSED TO BHS STANDARDS OF WEARABLE CUFFLESS BLOOD PRESSURE MONITORING

Index	Percentages			
	5 mmHg	8 mmHg	10 mmHg	15 mmHg
BHS (Grade A)	>60.00%	N/A	>85.00%	>95.00%
SBP	75.12%	85.07%	89.55%	95.02%
DBP	85.82%	93.53%	96.52%	99.25%

The bold values represent the best performance among the compared results.

demonstrate the ME and SD for SBP as 0.56 and 6.40 mmHg, respectively, and for DBP as 0.11 and 3.88 mmHg, respectively. These findings support the advantage of employing separate dense layers for SBP and DBP over a single-layer approach. The pre-trained model, incorporating personal information, not only demonstrates stronger correlations but also showcases more accurate predictions, as indicated by lower ME and SD values. The improved performance of the dual-layer architecture, particularly in capturing discrepancy in nature between SBP and DBP, highlights its efficacy in mitigating the challenges posed by the significant data range gap between these parameters. Given the significantly better performance of the pre-trained model utilizing personal information, it was selected as the foundation for subsequent transfer learning enhancements. Furthermore, the performance evaluation with the inclusion of personal information and separate dense layers was conducted using K-fold cross-validation, selecting the optimal K value to present the results of blood pressure prediction. This validation process further solidifies the reliability of the model. Across all the folds with K set to 5, the average ME was calculated at 0.66 mmHg for SBP and 13.14 mmHg for DBP, with corresponding average SDs of 5.76 mmHg for SBP and 10.19 mmHg for DBP. Such consistent performance underscores the robustness of the model and affirms its suitability for subsequent transfer learning enhancements.

With the model incorporating personal information used as in building the pre-trained model, the achieved MAEs and SDs comply to the required precision for Grade A of British Hypertension Society (BHS) [53]. To further explore the performance, Table II lists distribution percentages of errors within 5, 8, 10 and 15 mmHg, where it is seen that those within 8 mmHg (for Grade A [53]) are as high as 85.07% and 93.53%, respectively, for SBP and DBP. Next, to validate the architecture of our proposed DL

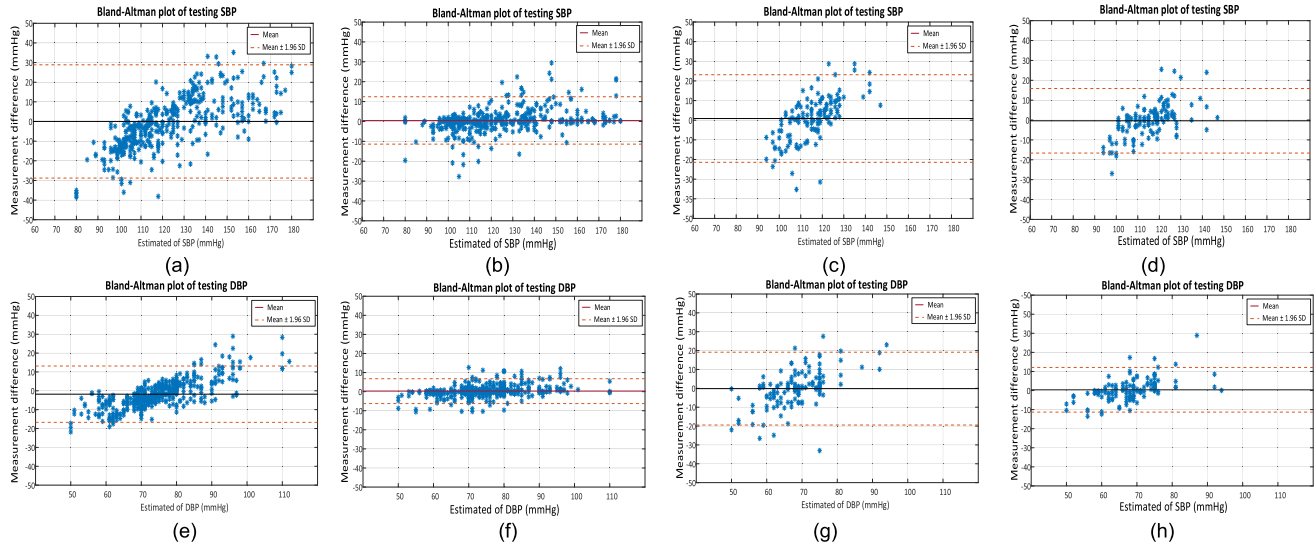


**Fig. 8.** Bland-Altman plots for SBP predictions presented in the upper series for (a) the baseline model without personal information, (b) the baseline model with personal information, (c) model trained exclusively based on pregnant women's database, and (d) finetuned model using pregnant women's database based on baseline training, (e) the baseline model without personal information, (f) the baseline model with personal information, (g) model trained exclusively on pregnant women's database, and (h) the fine-tuned model using pregnant women's database based on baseline training of the best cross-validation results.

**TABLE III**  
RESULTED MEAN ABSOLUTE ERRORS WITH DIFFERENT COMBINATIONS OF GRU AND CNN LAYERS IN THE BASELINE MODEL

			Unit: mmHg				
			1 CNN	2 CNN	3 CNN	4 CNN	5 CNN
4 GRU	Strided	SBP	4.46	4.52	5.10	5.234	6.30
		DBP	2.53	2.83	2.78	2.839	3.43
	Max-pooling	SBP	4.80	4.74	5.13	5.66	5.70
		DBP	2.81	2.91	2.78	3.119	3.04
3 GRU	Strided	SBP	4.57	<b>3.78</b>	4.56	4.786	5.80
		DBP	2.68	<b>2.29</b>	2.80	2.97	3.75
	Max-pooling	SBP	4.81	4.50	4.56	4.924	5.91
		DBP	2.60	2.52	2.54	2.924	3.52
2 GRU	Strided	SBP	5.23	6.28	5.56	5.912	6.38
		DBP	3.43	3.85	3.33	3.577	3.99
	Max-pooling	SBP	5.56	6.41	5.55	5.579	4.87
		DBP	3.23	3.42	3.41	3.177	2.88

The bold values represent the best performance among the compared results.

model in Fig. 6, varied configuration and sizes of the proposed DL model are considered. Table III presents the comparison in terms of the accuracy with varied combinations of CNN and GRU layers, showing that the 2-CNN-3-GRU model arrive at the lowest errors with a strided convolution approach. This finding underscores the effectiveness of this specific model setup in optimizing performance. This configuration was selected not only for its ability to minimize errors in the model's predictions but also for its potential to improve performance in personalized settings in the 3<sup>rd</sup> stage of model build-up. Further examination on the performance of the built model is presented in Table IV, which demonstrates well its superior performance in terms of standard deviations when compared to other deep learning architectures. On other hand, the results in Table V indicate that with 2-cycle PPG inputs, the model outperforms the others, as

three consecutive periods of qualified PPG waveforms measured are usually unstable in practice.

### B. Result of the Fine-Tuned Model for Pregnant Women Only

The baseline model was further fine-tuned by transfer learning based on the PPG dataset of pregnant women only. Its prediction on BP is next evaluated by resulted error distribution and SD/MAE. Table VI details the error distribution of sampled data in percentages within selected limits. It is seen clearly from this Table that the resulted errors of BP prediction rendered by the fine-tuned model comply well with those set up by the British Hypertension Society (BHS) in grade-B standards. On the other hand, listed in Table VII are resulted SDs and MAEs, where the built fine-tuned model via transfer learning delivers an SD of 7.15 mmHg for SBP and an MAE of 5.30 mmHg, as opposed to much higher SD of 8.89 mmHg and MAE of 6.10 mmHg precipitated without transfer learning by the baseline model built upon generic, normal people (i.e., the pre-train model in Fig. 5). As for DBP, the fine-tuned model also renders much better results with an SD of 5.06 mmHg for SBP and an MAE of 3.65 mmHg as opposed to a much higher SD of 7.62 mmHg and MAE of 6.23 mmHg by the baseline model. The correlation plot for this fine-tuned model via transfer learning is depicted in Fig. 7(d), while the Bland-Altman plots for SBP and DBP are in Fig. 8(d), (h), respectively. Notably again, the fine-tuned model's SD and MAE for SBP improved from 8.89 to 7.15 mmHg and from 6.10 to 5.30 mmHg, respectively, thanks to transfer learning, while for DBP from 7.62 to 5.06 mmHg in SD while from 6.23 to 3.65 mmHg in MAE. Such substantial improvement reflects the precision-enhancing capability of transfer learning from the baseline model as opposed to train merely use the baseline model.

**TABLE IV**  
PERFORMANCE COMPARISON OF BLOOD PRESSURE PREDICTION MODELS AMONG VARIED ARCHITECTURE COMBINATIONS

Architecture of the model					Unit: mmHg			
					Blood Pressure	ME	SD	MAE
1D-CNN	CBAM	GRU	LSTM	Attention	SBP	<b>0.56</b>	<b>6.40</b>	<b>3.78</b>
V	V	V	-	V	DBP	<b>0.11</b>	<b>3.88</b>	<b>2.29</b>
					SBP	0.33	7.63	5.01
V	V	-	V	V	DBP	0.05	4.98	3.16
					SBP	-0.34	7.85	5.44
V	-	V	-	V	DBP	0.05	4.75	3.11
					SBP	0.32	8.94	5.41
V	-	-	-	-	DBP	0.03	5.08	3.11
					SBP	0.66	7.53	5.78
V	-	-	-	-	DBP	-0.63	4.53	3.34

Note: In the “Architecture of the model,” ‘V’ indicates the inclusion of the respective layer in the model configuration for that experiment, while a ‘-’ indicates its exclusion.”

The bold values represent the best performance among the compared results.

**TABLE V**  
PERFORMANCE COMPARISON AMONG DIFFERENT NUMBERS OF COMPLETED PPG CYCLES IN BLOOD PRESSURE PREDICTION MODELS

		Unit: mmHg		
		ME	SD	MAE
Using 1 cycles	SBP	-0.56	10.75	7.02
	DBP	-0.10	6.10	3.94
Using 2 cycles	SBP	<b>0.56</b>	<b>6.40</b>	<b>3.78</b>
	DBP	<b>0.11</b>	<b>3.88</b>	<b>2.29</b>
Using 3 cycles	SBP	0.80	11.26	5.67
	DBP	0.14	4.96	2.58

The bold values represent the best performance among the compared results.

**TABLE VI**  
RESULTED DISTRIBUTION PERCENTAGES OF DATA BY THE FINE-TUNED MODEL AS OPPOSED TO BHS STANDARDS FOR WEARABLE CUFFLESS BLOOD PRESSURE

Item	Percentages			
	5 mmHg	8mmHg	10mmHg	15mmHg
BHS (Grade B)	>50%	N/A	>75%	>90%
SBP	57.26%	79.03%	85.48%	93.55%
DBP	75.00%	91.94%	94.35%	97.58%

The bold values represent the best performance among the compared results.

### C. Result of the Personalized Models for Individual Pregnant Women

The established fine-tuned model for pregnant women is next personalized further via multiple rounds of transfer learning based on personal PPGs measured by the patch in Fig. 1 and ground-truth BPs measured by cuff-type BP monitor [28]. Three women participated in building their individual personalized BP models. For each woman, 30 samples of PPG and ground-truth BPs are measured for building personalized BP models.

**TABLE VII**  
COMPARATIVE ANALYSIS IN ERRORS OF BLOOD PRESSURE PREDICTION FOR THE CASES WITH AND WITHOUT TRANSFER LEARNING

		Unit: mmHg		
		ME	SD	MAE
S	Without transfer learning	3.94	8.89	6.10
	With transfer learning	<b>-1.40</b>	<b>7.15</b>	<b>5.30</b>
D	Without transfer learning	3.89	7.62	6.23
	With transfer learning	<b>-0.44</b>	<b>5.06</b>	<b>3.65</b>

The bold values represent the best performance among the compared results.

**TABLE VIII**  
COMPARISON IN MEAN ABSOLUTE ERRORS TOWARDS THE BEST PERFORMING PERSONALIZED MODELS FOR BLOOD PRESSURE PREDICTION OF PREGNANT WOMEN

	Unit: mmHg					
	MAE of the baseline model	MAE of the finetuned model	MAE of the personalized model	MAE of the baseline model	MAE of the finetuned model	MAE of the personalized model
Pregnant women	SBP	DBP	SBP	DBP	SBP	DBP
1	4.15	2.07	4.91	6.20	<b>2.11</b>	<b>2.30</b>
2	3.10	5.74	2.19	2.83	<b>3.04</b>	<b>2.66</b>
3	2.60	19.47	1.29	3.66	<b>1.01</b>	<b>1.54</b>

The bold values represent the best performance among the compared results.

Table VIII presents MAEs resulted from the predicted blood pressure results using the baseline model, fine-tuned model for women only, and finally the personalized model. The errors exhibit decreasing trends from the baseline, fine-tuned to the personalized models, despite few errors increased from the baseline to the fine-tuned models. This is attributed to the

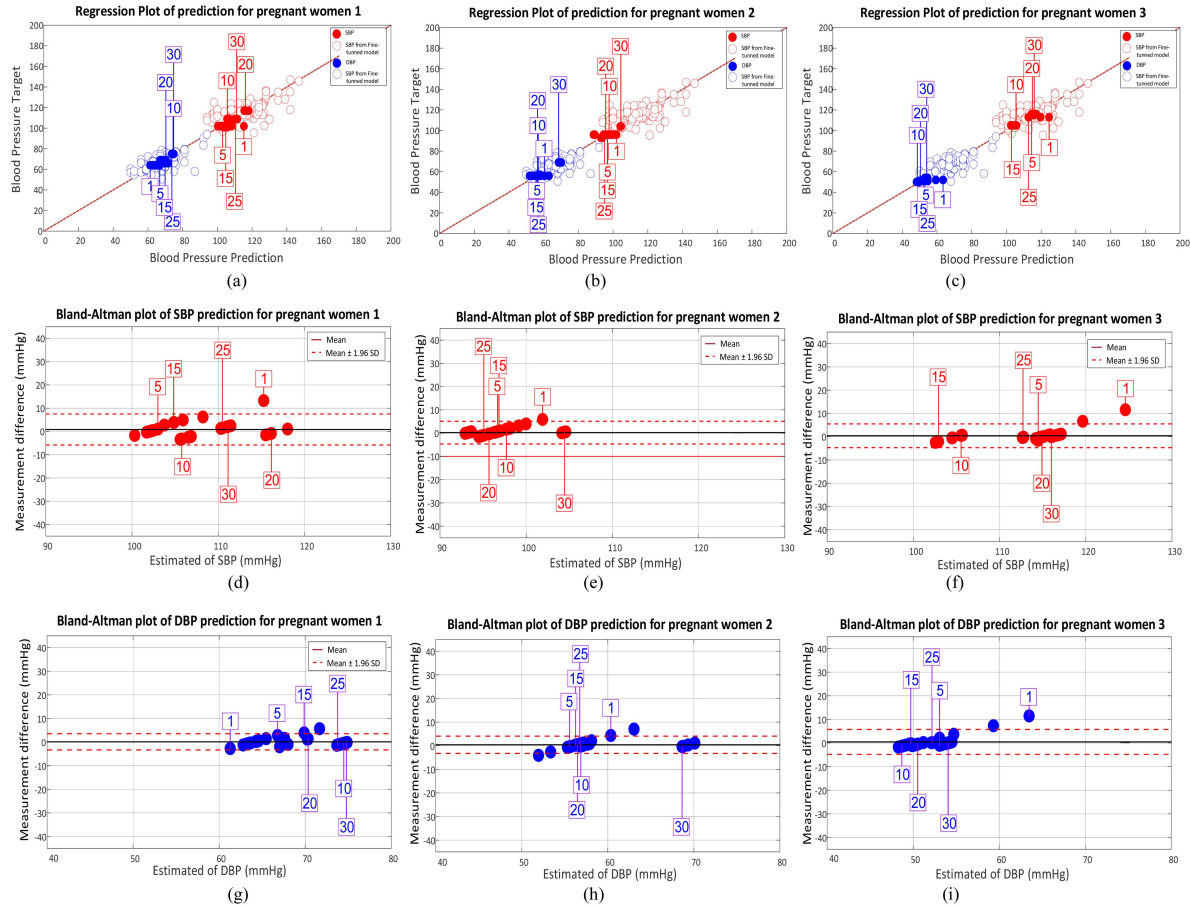


**Fig. 9.** Performance of the personalized models for SBP and DBP predictions for three pregnant women: (a)–(c) correlation plots of predictions for pregnant women 1–3, with numbered boxes corresponding to sequenced measurements; (d)–(f) bland-altman plot of SBP prediction for pregnant women 1–3, with numbered boxes denoting measured time points; (g)–(i) bland-altman plot of DBP prediction for pregnant women 1–3, with numbered boxes corresponding to sequenced measurements.

**TABLE IX**  
MEAN ERRORS AND STANDARD DEVIATIONS ( $ME \pm SD$ ) OF ERRORS BY THE BEST PERFORMING MODELS

Model	Baseline model		Fine-tuned model		Personalized model	
	SBP	DBP	SBP	DBP	SBP	DBP
1	$3.71 \pm 4.34$	$-19.1 \pm 2.11$	$4.20 \pm 3.52$	$5.61 \pm 3.69$	<b><math>-2.27 \pm 2.43</math></b>	<b><math>-0.92 \pm 2.90</math></b>
2	$-12.00 \pm 2.06$	$-26.4 \pm 2.96$	$1.85 \pm 1.84$	$2.69 \pm 1.45$	<b><math>0.16 \pm 1.75</math></b>	<b><math>-0.69 \pm 1.53</math></b>
3	$14.50 \pm 5.84$	$-9.63 \pm 7.19$	$-0.43 \pm 1.52$	$-3.67 \pm 1.58$	<b><math>-0.17 \pm 1.45</math></b>	<b><math>0.27 \pm 0.64</math></b>

The bold values represent the best performance among the compared results.

insufficient data used in the fine-tuned model as both baseline and fine-tuned models did not consider the data from the three pregnant women for training and testing. This is to ensure that the process of data splitting for different study stages has been clarified to ensure transparency and address concerns about potential data leakage. Each patient's data, consisting of three measurements, was exclusively assigned to either the training or testing set. This approach mitigates the risk of bias introduced by inherent patterns in measurements from the same individuals. As the relationship between PPG signals and blood pressure values differs among pregnant women, it is normal for data

from pregnant women who were not included in the training database to have sub-optimal results. This emphasizes however the importance of using a personalized model.

The performance of predicting BP by the built personalized models for the three pregnant women is shown in Fig. 9 via correlations in (a-c), Bland-Altman in (d-f) for SBP and (g-i) for DBPs. The numeric labels refer to how many sets of collected PPG and ground-truths have been used for transfer learnings. It is clearly seen from the correlations in Bland-Altman in (d-f) that the predicted BPs clustered near the zero mean difference, the solid lines in all subfigure, as the number of sets of collected

**TABLE X**  
COMPARATIVE ANALYSIS ON BLOOD PRESSURE PREDICTION BY RECENT STUDIES AND THE PROPOSED

Year	Author(s)	Approach	Database	Blood Pressure	ME	SD	MAE	
2019	S. Baek, J. Jang and S. Yoon [54]	CNN	MIMIC dataset (PPG)	SBP	-1.29	7.58	5.32	
				DBP	-0.48	5.08	3.38	
2020	M. Panwar, A. Gautam, D. Biswas and A. Acharyya [55]	CNN-LSTM	MIMIC dataset (PPG)	SBP	1.55	5.41	4.034	
				DBP	-1.25	5.65	2.50	
2021	C. E. Hajj and P. A. Kyriacou [56]	GRU	MIMIC dataset (PPG)	SBP	-1.24	8.52	5.77	
				DBP	-0.44	5.02	3.33	
2022	H. Samimi and H. R. Dajani [57]	ANN	MIMIC dataset (PPG)	SBP	-1.17	16.86	13.97	
				DBP	-0.70	7.16	5.85	
2022	S. Haddad, A. Boukhayma and A. Caizzone [58]	Multi-Linear Regression	MIMIC dataset (PPG)	SBP	-	-	6.10	
				DBP	-	-	4.65	
2022	W. Wang, P. Mohseni, K. L. Kilgore and L. Najafizadeh [59]	CNN	MIMIC dataset (PPG)	SBP	-0.00	8.46	6.17	
				DBP	-0.04	5.36	3.66	
2022	Y. Zhang, X. Ren, X. Liang [60]	BiLSTM-attention	MIMIC dataset (PPG)	SBP	-	4.04	2.81	
				DBP	-	2.98	1.87	
2022	J. Leitner, P. -H. Chiang and S. Dey [61]	BP-CRNN Layers Personalized Model	MIMIC dataset (PPG)	SBP	-	-	4.47	
				DBP	-	-	3.18	
2023	Shirong Qiu, <i>et al.</i> [22]	Scenario-adaptive pattern-fusion	MIMIC dataset (PPG)	SBP	-	3.81	6.84	
				DBP	-	5.00	8.83	
2023	Chenbin Ma, <i>et al.</i> [21]	Knowledge distillation informer	Private and MIMIC dataset (PPG)	SBP	0.02	5.93	-	
				DBP	0.01	3.87	-	
2023	Proposed	Proposed model	MIMIC dataset	SBP	0.70	5.32	5.86	
		Proposed baseline model	Self-collected dataset of 154 normal people (PPG)	DBP	0.24	2.97	2.90	
				SBP	<b>0.56</b>	<b>6.40</b>	<b>3.78</b>	
				DBP	<b>0.11</b>	<b>3.88</b>	<b>2.29</b>	
		Fine-tuned model by the data of pregnant women only	Self-collected dataset of 40 pregnant women (PPG)	SBP	With transfer learning	<b>-1.40</b>	<b>7.15</b>	<b>5.30</b>
					Without transfer learning	3.94	8.89	6.10
				DBP	With transfer learning	<b>-0.44</b>	<b>5.06</b>	<b>3.65</b>
					Without transfer learning	3.89	7.62	6.23
		Personalized Model based on fine-tuned model		SBP	<b>-0.17</b>	<b>1.45</b>	<b>0.98</b>	
				DBP	<b>0.27</b>	<b>0.64</b>	<b>0.43</b>	

The bold values represent the best performance among the compared results.

PPG and ground-truths used for transfer learning increases from 1 to 30, indicating a significant improvement over the increased sets of collected PPG and ground-truths, and of course showing high accuracies that can be achieved by personalization based on a number of sets of PPG and ground-truths for a single subject. This improvement and final high accuracies are well observed across all three pregnant women. In addition to graphical presentation in Fig. 9, the numerical MEs and SDs resulted are listed in Table IX to explore further the performance of the built personalized BP models. For pregnant woman 1, the personalized model achieves an accuracy of  $-2.27(\text{ME})\pm 2.43(\text{SD})$  for SBP while  $-0.92\pm 2.90$  for DBP. For woman 2, the model yields an ME of  $0.16\pm 1.75$  for SBP and  $-0.69\pm 1.53$  for DBP. Woman 3 leads to an ME of  $\mathbf{-0.17\pm 1.45}$  for SBP and  $\mathbf{0.27\pm 0.64}$  for DBP. It is evident that both MEs and SDs of all 3 women resulted from the personalized model are lower than both the baseline and fine-tune models, indicating favorable accuracy and precision delivered by the personalized model for predicting BPs. It demonstrates well a potential of increasing the number of datasets of measured PPG and ground-truths to obtain precision BP prediction for a given pregnant women. Note herein that

the performance of personalization is demonstrated by 3-only pregnant women. The effectiveness of this proposed personalization can be further affirmed by much data collected from more pregnant women in the future.

#### D. Performance Evaluation and Discussion

Effort is paid next to confirm that the designed architecture and size in the model in Fig. 6 is superior to many other deep-learning models in different architectures and sizes based in-depth discussion. The performances of using different numbers of CNN and GRU layers in DL model are detailed in Table III, where different results of whether using a strided or a max pooling layer are also compared. Seen in this table, a strided 2-CNN-3-GRU model has performs the best, i.e., the lowest errors. To explore further the performance of this 2-CNN-3-GRU model, Table IV shows the comparison in performance among different types of deep learning architectures, showing the proposed one in Fig. 6 deliver the lowest SDs. Table V compares the performances of using different numbers of PPG cycles in measured PPG waveforms and different samples to the model as inputs. It shows that the 2-cycle inputs lead to the best performance, as

consecutive 3 periods of a qualified PPG waveform are more challenging to obtain. Moreover, this analysis on input cycle selection highlights also the advantage of using a certain number of PPG cycles, which balances performance with practicality in data collection.

The proposed model is also evaluated based on the comparison to prior arts in Table X with metrics of ME, SD and MAE. Shown in this table, the proposed DL model built upon MIMIC database delivers an SD for SBP being 5.32 mmHg, while SD for DBP at 2.97 mmHg. Moreover, the MAE for SBP is 5.86 mmHg, while for DBP, 2.90 mmHg. These metric values collectively show the effectiveness of the built model in achieving robust performance, comparable to other studies. However, a notable challenge arises regarding SD, particularly in predicting DBP. Some prior models exhibit lower SD values for DBP than the proposed model, as low as 2.97 mmHg, indicating slightly superior performance in this regard. Nevertheless, when applied to the MIMIC dataset, the proposed model's SD for DBP stands out as achieving the best performance as compared to all the other prior studies. Moreover, general low error metric values resulted from the proposed model are seen in Table X, compared to other studies that employ rather typical CNN, ANN, or other machine learnings without transfer learning. Furthermore, with transfer learning conducted from the baseline model, the fine-tuned model shows an improved performance for pregnant women. The fine-tuned model's SD and MAE for SBP are improved from 8.89 to 7.15 mmHg and from 6.10 to 5.30 mmHg, respectively, thanks to transfer learning, while for DBP from 7.62 to 5.06 mmHg in SD and from 6.23 to 3.65 mmHg in MAE.

The personalized models, built in the 3<sup>rd</sup> stage using transfer learning again for individual pregnant women, demonstrate even much improvements, with the lowest SD and MAE, 1.45 and 0.98 mmHg for SBP, respectively, while 0.64 and 0.43 mmHg for DBP, respectively, better than all others in Table X. These results highlight the proposed approach's efficacy in enhancing the accuracy of BP predictions for individual pregnant women, outperforming existing methods that rely on CNN, ANN, or other conventional machine learning techniques. The achieved performance attributes largely to the consideration of individual woman's physiological characteristics by personalization. The personalized models would be advantageous in clinical practice for monitoring blood pressure continuously during pregnancy, particularly for the case when wearable PPG device users can provide few sets of PPG and ground-truth data for personalization.

#### IV. CONCLUSION

Deep learning models in 3 stages were successfully built to predict well the blood pressures for pregnant women to deliver effective pre-warning of pre-eclampsia. The first model is a pre-trained, baseline deep learning (DL) model that utilizes the PPG data at large to create the base weights for the BP model, achieving a high performance with  $0.56$  (mean error)  $\pm$   $6.04$  (standard deviation) for SBP and  $0.11 \pm 3.88$  for DBP. The second is another DL model that was built from fine-tuning the

baseline model by limited data of pregnant women, resulting in better accuracy with  $-1.40 \pm 7.15$  for SBP and  $-0.44 \pm 5.06$  for DBP. The third type of models are the personalized models for 3 individual pregnant women, which were developed using the transfer learnings again, arriving at even better precisions, with  $-0.17$  (mean error)  $\pm$   $1.45$  (standard deviation) for SBP and  $0.27 \pm 0.64$  for DBP. Despite the success herein, measuring PPG data with adequate quality can be challenging due to interference from ambient light and motion artifacts resulting from subject movement. Future efforts will be focused on developing algorithms to reduce the impact of ambient lighting and motion artifacts in real-time, with the aim of facilitating easier and more accurate blood pressure measurements for pregnant women. Lastly, note that this study was limited to a single site and a small sample size of pregnant women for fine-tuning and personalization; hence, future effort would involve a larger sample size from multiple sites to validate the generalizability and applicability of these models.

#### REFERENCES

- [1] J. M. Roberts and H. S. Gammill, "Preeclampsia: Recent insights," *Hypertension*, vol. 46, no. 6, pp. 1243–1249, Dec. 2005, doi: [10.1161/01.HYP.0000188408.49896.c5](https://doi.org/10.1161/01.HYP.0000188408.49896.c5).
- [2] J. G. L. Ramos, N. Sass, and S. H. M. Costa, "Preeclampsia," *Revista Brasileira de Ginecologia E Obstetricia*, vol. 39, no. 9, pp. 496–512, Sep. 2017, doi: [10.1055/s-0037-1604471](https://doi.org/10.1055/s-0037-1604471).
- [3] S. Rana, E. Lemoine, J. P. Granger, and S. A. Karumanchi, "Preeclampsia: Pathophysiology, challenges, and perspectives," *Circulation Res.*, vol. 124, no. 7, pp. 1094–1112, Mar. 2019, doi: [10.1161/CIRCRESAHA.118.313276](https://doi.org/10.1161/CIRCRESAHA.118.313276).
- [4] E. Eiland, C. Nzerue, and M. Faulkner, "Preeclampsia 2012," *J. Pregnancy*, vol. 2012, 2012, Art. no. 586578, doi: [10.1155/2012/586578](https://doi.org/10.1155/2012/586578).
- [5] L. C. Chesley, "History and epidemiology of preeclampsia-eclampsia," *Clin. Obstet. Gynecol.*, vol. 27, no. 4, pp. 801–820, Dec. 1984, doi: [10.1097/00003081-198412000-00004](https://doi.org/10.1097/00003081-198412000-00004).
- [6] G. Mancia et al., "Effects of blood-pressure measurement by the doctor on patient's blood pressure and heart rate," *Lancet*, vol. 2, no. 8352, pp. 695–698, Sep. 1983, doi: [10.1016/s0140-6736\(83\)92244-4](https://doi.org/10.1016/s0140-6736(83)92244-4).
- [7] C. E. Clark, I. A. Horvath, R. S. Taylor, and J. L. Campbell, "Doctors record higher blood pressures than nurses: Systematic review and meta-analysis," *Brit. J. Gen. Pract.*, vol. 64, no. 621, pp. e223–e232, 2014.
- [8] G. Parati et al., "Evaluation of the baroreceptor-heart rate reflex by 24-hour intra-arterial blood pressure monitoring in humans," *Hypertension*, vol. 12, no. 2, pp. 214–222, 1988.
- [9] P. Little, J. Barnett, L. Barnsley, J. Marjoram, A. Fitzgerald-Barron, and D. Mant, "Comparison of agreement between different measures of blood pressure in primary care and daytime ambulatory blood pressure," *Bmj*, vol. 325, no. 7358, 2002, Art. no. 254.
- [10] G. C. Roush et al., "Prognostic impact from clinic, daytime, and night-time systolic blood pressure in nine cohorts of 13 844 patients with hypertension," *J. Hypertension*, vol. 32, no. 12, pp. 2332–2340, 2014.
- [11] R. H. Fagard et al., "Daytime and nighttime blood pressure as predictors of death and cause-specific cardiovascular events in hypertension," *Hypertension*, vol. 51, no. 1, pp. 55–61, 2008.
- [12] A. Hurrell, L. Webster, L. C. Chappell, and A. H. Shennan, "The assessment of blood pressure in pregnant women: Pitfalls and novel approaches," *Amer. J. Obstet. Gynecol.*, vol. 226, no. 2, pp. S804–S818, 2022.
- [13] J. R. Higgins and M. de Swiet, "Blood-pressure measurement and classification in pregnancy," *Lancet*, vol. 357, no. 9250, pp. 131–135, 2001.
- [14] M. A. Brown, L. Reiter, B. Smith, M. L. Buddle, R. Morris, and J. A. Whitworth, "Measuring blood pressure in pregnant women: A comparison of direct and indirect methods," *Amer. J. Obstet. Gynecol.*, vol. 171, no. 3, pp. 661–667, 1994.
- [15] Y. Gupta, S. Kumar, and V. Mago, "Pregnancy health monitoring system based on biosignal analysis," in *Proc. IEEE 42nd Int. Conf. Telecommun. Signal Process.*, 2019, pp. 664–667.

- [16] J. Fine et al., "Sources of inaccuracy in photoplethysmography for continuous cardiovascular monitoring," *Biosensors*, vol. 11, no. 4, 2021, Art. no. 126.
- [17] S. Tian, W. Yang, J. M. Le Grange, P. Wang, W. Huang, and Z. Ye, "Smart healthcare: Making medical care more intelligent," *Glob. Health J.*, vol. 3, no. 3, pp. 62–65, 2019.
- [18] H. W. Loh et al., "Application of photoplethysmography signals for health-care systems: An in-depth review," *Comput. Methods Programs Biomed.*, vol. 216, 2022, Art. no. 106677.
- [19] P. Kaushik and P. Sethi, "A comprehensive study on blood pressure measurement techniques," in *Proc. IEEE 4th Int. Conf. Comput. Commun. Automat.*, 2018, pp. 1–3.
- [20] M. Thiga, P. Kimeto, M. Mgala, E. Kweyu, S. Wanyee, and T. Mwirigi, "A remote blood pressure data collection and monitoring system for expectant mothers," in *Proc. IST-Afr. Conf.*, 2022, pp. 1–9.
- [21] C. Ma et al., "KD-Informer: Cuff-less continuous blood pressure waveform estimation approach based on single photoplethysmography," *IEEE J. Biomed. Health Inform.*, vol. 27, no. 5, pp. 2219–2230, May 2023.
- [22] S. Qiu, Y.-T. Zhang, S.-K. Lau, and N. Zhao, "Scenario adaptive cuffless blood pressure estimation by integrating cardiovascular coupling effects," *IEEE J. Biomed. Health Inform.*, vol. 27, no. 3, pp. 1375–1385, Mar. 2022.
- [23] X. Chang, G. Li, G. Xing, K. Zhu, and L. Tu, "DeepHeart: A deep learning approach for accurate heart rate estimation from PPG signals," *ACM Trans. Sensor Netw.*, vol. 17, no. 2, pp. 1–18, 2021.
- [24] S. Ismail, I. Siddiqi, and U. Akram, "Heart rate estimation in PPG signals using convolutional-recurrent regressor," *Comput. Biol. Med.*, vol. 145, 2022, Art. no. 105470.
- [25] Z. Sun, J. Junntila, M. Tulppo, T. Seppänen, and X. Li, "Non-contact atrial fibrillation detection from face videos by learning systolic peaks," *IEEE J. Biomed. Health Inform.*, vol. 26, no. 9, pp. 4587–4598, Sep. 2022.
- [26] J. Ramesh, Z. Solatidehkordi, R. Aburukba, and A. Sagahyroon, "Atrial fibrillation classification with smart wearables using short-term heart rate variability and deep convolutional neural networks," *Sensors*, vol. 21, no. 21, 2021, Art. no. 7233.
- [27] R. K. Pandey and P. C.-P. Chao, "A dual-channel ppg readout system with motion-tolerant adaptability for oled-opd sensors," *IEEE Trans. Biomed. Circuits Syst.*, vol. 16, no. 1, pp. 36–51, Feb. 2022.
- [28] "OMRON healthcare, inc," 2019. [Online]. Available: <https://omronhealthcare.com/products/5-series-upper-arm-blood-pressure-monitor-bp7200/>
- [29] D. H. Nguyen, P. C.-P. Chao, H.-H. Shuai, Y.-W. Fang, and B. S. Lin, "Achieving high accuracy in predicting blood flow volume at the arteriovenous fistulas of hemodialysis patients by intelligent quality assessment on PPGs," *IEEE Sensors J.*, vol. 22, no. 6, pp. 5844–5856, Mar. 2022.
- [30] R. Yousefi, M. Nourani, and I. Panahi, "Adaptive cancellation of motion artifact in wearable biosensors," in *Proc. IEEE Annu. Int. Conf. Eng. Med. Biol. Soc.*, 2012, pp. 2004–2008.
- [31] S. H. Kim, D. W. Ryoo, and C. Bae, "Adaptive noise cancellation using accelerometers for the PPG signal from forehead," in *Proc. IEEE 29th Annu. Int. Conf. Eng. Med. Biol. Soc.*, 2007, pp. 2564–2567.
- [32] S. Li, L. Liu, J. Wu, B. Tang, and D. Li, "Comparison and noise suppression of the transmitted and reflected photoplethysmography signals," *BioMed Res. Int.*, vol. 2018, 2018, Art. no. 4523593.
- [33] D. Ban and S. Kwon, "Movement noise cancellation in PPG signals," in *Proc. IEEE Int. Conf. Consum. Electron.*, 2016, pp. 47–48.
- [34] S.-M. Kim, E.-J. Cha, D.-W. Kim, J.-H. Yoo, D.-Y. Kim, and S.-C. Kim, "Noise reduction of PPG signal during free movements using adaptive SFLC (Scaled Fourier Linear Combiner)," *Trans. Korean Inst. Elect. Engineers D*, vol. 55, no. 3, pp. 138–141, 2006.
- [35] C. El-Hajj and P. A. Kyriacou, "Deep learning models for cuffless blood pressure monitoring from PPG signals using attention mechanism," *Biomed. Signal Process. Control*, vol. 65, 2021, Art. no. 102301.
- [36] Y.-H. Kao, P. C.-P. Chao, and C.-L. Wey, "Design and validation of a new PPG module to acquire high-quality physiological signals for high-accuracy biomedical sensing," *IEEE J. Sel. Topics Quantum Electron.*, vol. 25, no. 1, pp. 1–10, Jan./Feb. 2019.
- [37] S. Mahmud et al., "A shallow U-net architecture for reliably predicting blood pressure (BP) from photoplethysmogram (PPG) and electrocardiogram (ECG) signals," *Sensors*, vol. 22, no. 3, 2022, Art. no. 919.
- [38] H. Asada, A. Reisner, P. Shaltis, and D. McCombie, "Towards the development of wearable blood pressure sensors: A photo-plethysmograph approach using conducting polymer actuators," in *Proc. IEEE Eng. Med. Biol. 27th Annu. Conf.*, 2005, pp. 4156–4159.
- [39] S. Puranik and A. W. Morales, "Heart rate estimation of PPG signals with simultaneous accelerometry using adaptive neural network filtering," *IEEE Trans. Consum. Electron.*, vol. 66, no. 1, pp. 69–76, Feb. 2020.
- [40] Y. Liang, M. Elgendi, Z. Chen, and R. Ward, "An optimal filter for short photoplethysmogram signals," *Sci. Data*, vol. 5, no. 1, pp. 1–12, 2018.
- [41] A. Chatterjee and U. K. Roy, "PPG based heart rate algorithm improvement with Butterworth IIR filter and Savitzky-Golay FIR filter," in *Proc. IEEE 2nd Int. Conf. Electron., Mater. Eng. Nano-Technol.*, 2018, pp. 1–6.
- [42] S. A. Akar, S. Kara, F. Latifoğlu, and V. Bilgic, "Spectral analysis of photoplethysmographic signals: The importance of preprocessing," *Biomed. Signal Process. Control*, vol. 8, no. 1, pp. 16–22, 2013.
- [43] M. Z. Suboh, R. Jaafar, N. A. Nayan, N. H. Harun, and M. S. F. Mohamad, "Analysis on four derivative waveforms of photoplethysmogram (PPG) for fiducial points detection," *Front Public Health*, vol. 10, 2022, Art. no. 920946.
- [44] R. M. Rozi, M. M. Ali, and M. B. I. Reaz, "Effects of exercise on the second derivative photoplethysmography (PPG) waveform," in *Proc. IEEE Asia Pacific Conf. Circuits Syst.*, 2010, pp. 804–807.
- [45] M. S. S. Johnson and J. M. Eklund, "A review of photoplethysmography-based physiological measurement and estimation, part 2: Multi-input methods," in *Proc. IEEE 42nd Annu. Int. Conf. Eng. Med. Biol. Soc.*, 2020, pp. 863–866.
- [46] D. Fujita and A. Suzuki, "Evaluation of the possible use of PPG waveform features measured at low sampling rate," *IEEE Access*, vol. 7, pp. 58361–58367, 2019.
- [47] S. Woo, J. Park, J.-Y. Lee, and I. S. Kweon, "CBAM: Convolutional block attention module," in *Proc. Eur. Conf. Comput. Vis.*, 2018, pp. 3–19.
- [48] A. Vaswani et al., "Attention is all you need," in *Proc. Adv. Neural Inf. Process. Syst.*, 2017, p. 1.
- [49] S. Zanelli, M. A. El Yacoubi, M. Hallab, and M. Ammi, "Transfer learning of CNN-based signal quality assessment from clinical to non-clinical PPG signals," in *Proc. IEEE 43rd Annu. Int. Conf. Eng. Med. Biol. Soc.*, 2021, pp. 902–905.
- [50] M. Strickert, F.-M. Schleif, T. Villmann, and U. Seiffert, "Unleashing pearson correlation for faithful analysis of biomedical data," in *Similarity-Based Clustering: Recent Developments and Biomedical Applications*. Berlin, Germany: Springer, 2009, pp. 70–91.
- [51] R. F. Woolson and W. R. Clarke, *Statistical Methods for the Analysis of Biomedical Data*. Hoboken, NJ, USA: Wiley, 2011.
- [52] O. Gerke, "Reporting standards for a Bland–Altman agreement analysis: A review of methodological reviews," *Diagnostics*, vol. 10, no. 5, 2020, Art. no. 334.
- [53] *IEEE standard for wearable cuffless blood pressure measuring devices*, IEEE Standard 1708-2014, pp. 1–38, Aug. 2014.
- [54] S. Baek, J. Jang, and S. Yoon, "End-to-end blood pressure prediction via fully convolutional networks," *IEEE Access*, vol. 7, pp. 185458–185468, 2019.
- [55] M. Panwar, A. Gautam, D. Biswas, and A. Acharyya, "PP-Net: A deep learning framework for PPG-based blood pressure and heart rate estimation," *IEEE Sensors J.*, vol. 20, no. 17, pp. 10000–10011, Sep. 2020.
- [56] C. El Hajj and P. A. Kyriacou, "Recurrent neural network models for blood pressure monitoring using PPG morphological features," in *Proc. IEEE 43rd Annu. Int. Conf. Eng. Med. Biol. Soc.*, 2021, pp. 1865–1868.
- [57] H. Samimi and H. R. Dajani, "Cuffless blood pressure estimation using cardiovascular dynamics," in *Proc. IEEE Int. Conf. Elect., Comput. Energy Technol.*, 2022, pp. 1–8.
- [58] S. Haddad, A. Boukhayma, and A. Caizzone, "Continuous PPG-based blood pressure monitoring using multi-linear regression," *IEEE J. Biomed. Health Inform.*, vol. 26, no. 5, pp. 2096–2105, 2021.
- [59] W. Wang, P. Mohseni, K. L. Kilgore, and L. Najafizadeh, "Cuff-less blood pressure estimation from photoplethysmography via visibility graph and transfer learning," *IEEE J. Biomed. Health Inform.*, vol. 26, no. 5, pp. 2075–2085, 2022, doi: [10.1109/JBHI.2021.3128383](https://doi.org/10.1109/JBHI.2021.3128383).
- [60] Y. Zhang, X. Ren, X. Liang, X. Ye, and C. Zhou, "A refined blood pressure estimation model based on single channel photoplethysmography," *IEEE J. Biomed. Health Inform.*, vol. 26, no. 12, pp. 5907–5917, 2022.
- [61] J. Leitner, P.-H. Chiang, and S. Dey, "Personalized blood pressure estimation using photoplethysmography: A transfer learning approach," *IEEE J. Biomed. Health Inform.*, vol. 26, no. 1, pp. 218–228, 2021.